



## Airborne measurements indicate large methane emissions from the eastern Amazon basin

John B. Miller,<sup>1,2</sup> Luciana V. Gatti,<sup>3</sup> Monica T. S. d'Amelio,<sup>3</sup> Andrew M. Crotwell,<sup>1,2</sup> Edward J. Dlugokencky,<sup>1</sup> Peter Bakwin,<sup>1</sup> Paulo Artaxo,<sup>4</sup> and Pieter P. Tans<sup>1</sup>

Received 27 December 2006; revised 23 March 2007; accepted 24 April 2007; published 25 May 2007.

[1] Recent results from laboratory, field and remote sensing measurements suggest the presence of large methane emissions from the Amazon basin. Here we present regionally integrative, direct trace gas observations from two sites that confirm the presence of large fluxes of methane in eastern Amazônia. Air samples collected on aircraft near Santarém (2.9°S, 55.0°W) and Manaus (2.6°S, 60.0°W) in eastern and central Amazônia show large enhancements of CH<sub>4</sub> that are not seen at the NOAA/ESRL background sites in the tropical Atlantic Ocean. From the surface to about four km, enhancements averaging 34 ppb and up to 200 ppb occur throughout the year and we calculate emissions averaging 27 mg CH<sub>4</sub>/m<sup>2</sup>/day from upwind sources. **Citation:** Miller, J. B., L. V. Gatti, M. T. S. d'Amelio, A. M. Crotwell, E. J. Dlugokencky, P. Bakwin, P. Artaxo, and P. P. Tans (2007), Airborne measurements indicate large methane emissions from the eastern Amazon basin, *Geophys. Res. Lett.*, 34, L10809, doi:10.1029/2006GL029213.

### 1. Introduction

[2] Understanding methane growth rate variations and the processes responsible for them is difficult because of the wide variety of methane sources [Cicerone and Oremland, 1988] and the problem of distinguishing individual sources in the atmosphere even when using isotopes [Miller *et al.*, 2002]. Until recently, ESRL measurements have only been made in the tropical marine boundary layer (MBL), where they are largely decoupled from continental emissions. This greatly limits our ability to infer tropical CH<sub>4</sub> fluxes [e.g., Bousquet *et al.*, 2006; Houweling *et al.*, 1999].

[3] Retrievals of column-mean CH<sub>4</sub> mixing ratio from SCIAMACHY during 2003 and 2004 [Frankenberg *et al.*, 2006] show CH<sub>4</sub> abundances above the Amazon basin and other parts of northern South America substantially larger than expected from process-based model estimates of methane emission from wetlands [Walter *et al.*, 2001]. However, more recent estimates of Amazonian wetland emissions [Melack *et al.*, 2004] show more consistency with SCIAMACHY observations [Bergamaschi *et al.*, 2006]. Additionally, recent laboratory results [Keppler *et al.*, 2006] pointing to plants as direct emitters of methane and

field measurements from Amazonian upland forests [do Carmo *et al.*, 2006] suggest that sources other than wetlands may also be important contributors to Amazonian methane emissions.

[4] Here, we present a four year record of CH<sub>4</sub> vertical profiles from the surface to at least 3600 m (asl), above two sites in the central Amazon, near the cities of Santarém (SAN) and Manaus (MAN) (Figure 1). These data do not have the spatial and temporal density of the satellite columns, but are very accurate and precise and being direct measurements do not suffer from any of the biases of SCIAMACHY, including assumptions about CO<sub>2</sub> mixing ratios (to which SCIAMACHY CH<sub>4</sub> radiances are scaled) and aerosol contamination. SCIAMACHY also cannot reliably retrieve methane over the oceans, so that its marine – continental gradients are not well defined. We reference our Amazonian measurements to those made at our remote sampling sites at Ascension Island (ASC; 7.9°S, 14.4°W) and Barbados (RPB; 13.2°N, 59.4°W) located in the tropical Atlantic, because these sites represent air entering the Amazon basin through the trade winds. We will use enhancements of CH<sub>4</sub> at SAN or MAN relative to background to estimate the surface flux of CH<sub>4</sub> between Brazil's Atlantic coast and the sites.

### 2. Methods

[5] At SAN and MAN, air was collected with portable sampling systems consisting of separate compressor and flask units [Tans *et al.*, 1996]. These units are loaded onto a light aircraft, and the pilot initiates sample collection at pre-determined altitudes. Most flights consisted of one descending and one ascending profile from 3600 m to 300 m. From 2000 to 2003, samples collected in Brazil were sent to the NOAA lab in Boulder, USA, where they were analyzed for CO<sub>2</sub>, CH<sub>4</sub>, CO, N<sub>2</sub>O, SF<sub>6</sub>, and H<sub>2</sub>. Measurement repeatability for CH<sub>4</sub> is estimated to be better than 0.1% (<2 ppb, 1σ), and all CH<sub>4</sub> measurements reported here are on the NOAA2004 scale [Dlugokencky *et al.*, 2005]. Since 2004, a replica of the NOAA analysis system began operating in Brazil at Instituto de Pesquisas Energéticas e Nucleares (IPEN), with precision and accuracy very similar to that at NOAA. Air at ASC and RPB was sampled into 2.2 L glass flasks with Teflon-tipped glass stopcocks and filled to about 1.2 bar [Conway *et al.*, 1994], and shipped to NOAA for analysis of the same suite of gases. All measurements presented here are available via anonymous ftp at ftp.cmdl.noaa.gov/pub/LBA.

[6] At SAN, ascending profiles were made above the Tapajós National Forest, near the “km 67” tower that is located about 10 km to the east of the Tapajós river. For the

<sup>1</sup>NOAA Earth System Research Laboratory, Boulder, Colorado, USA.

<sup>2</sup>Cooperative Institute for Research in Environmental Sciences, University of Colorado, Boulder, Colorado, USA.

<sup>3</sup>Divisão de Química Ambiental, Laboratório de Química Atmosférica, Instituto de Pesquisas Energéticas e Nucleares, São Paulo, Brazil.

<sup>4</sup>Instituto de Física, Universidade de São Paulo, São Paulo, Brazil.

first 4 years, descending profiles were made 30 km to the east of the tower to evaluate possible impacts of fluxes from the river [Richey *et al.*, 2002]. At MAN, ascending profiles were made above the “K34” tower to the northwest of the city of Manaus (population 1.8 million), following descending profiles 50 km to the northeast of Manaus, in order to avoid possible pollution from Manaus at the K34 tower, which can be downwind of the city. At both SAN and MAN, differences between ascending and descending profiles were generally small compared to differences with ASC (Figure S1 of the auxiliary material),<sup>1</sup> so for our analysis, we use the vertically denser profiles above the towers at both sites, reserving the alternate profiles for sensitivity tests. Between 2000 and 2003, 11 vertical profiles were also conducted off the Atlantic coast of Brazil, 50 km NE of the city of Fortaleza (FTL, 4.15°S, 38.28°W) to sample air entering the Amazon basin.

### 3. Results and Discussion

[7] Air entering the Amazon basin is dominated by trade-wind easterlies coming from the tropical Atlantic Ocean, although the relative influence of Northern and Southern Hemisphere air depends upon the seasonally varying latitude of the ITCZ. Thus, the difference between our SAN and MAN measurements and the Atlantic background should be directly related to terrestrial CH<sub>4</sub> fluxes; oceanic CH<sub>4</sub> fluxes are assumed negligible as supported by the small differences between measurements at FTL and ASC (Figure 2). Until 2004, the vast majority of measurements took place during the wet season, but since that time there have been numerous dry season profiles. Large enhancements are evident in both seasons and there are no clear differences in the character of dry and wet season profiles. However, during the dry season, CO can also be significantly enhanced suggesting that elevated CH<sub>4</sub> in the same samples results from biomass burning. The ratio of CO to CH<sub>4</sub> enhancements relative to background ranges from 0.13 to 0.82 mol/mol in the wet season and 1.8 to 6.3 mol/mol during the dry season. A review of emission measurements [Andreae and Merlet, 2001] suggests a ratio of 9 mol/mol for tropical forest burning, roughly consistent with our observations.

[8] Figure 2 shows that CH<sub>4</sub> at SAN and MAN relative to ASC and RPB is almost always enhanced, thus indicating the presence of upwind sources. The largest enhancements are in the convective boundary layer (CBL), but enhancements in the free troposphere can also be seen in numerous profiles, possibly indicating the convective redistribution of methane emitted into the CBL. Because of strong convection one cannot count on surface emissions to be trapped in the CBL, so we do not calculate fluxes using a boundary layer budgeting technique [e.g., Lloyd *et al.*, 2001]. Instead, we use a column integration technique that does not distinguish the CBL and free troposphere.

[9] To apply this technique, we first determine the background CH<sub>4</sub> mixing ratio entering Brazil off the Atlantic Ocean. Because the relative Northern and Southern Hemisphere contributions to the CH<sub>4</sub> background vary, we

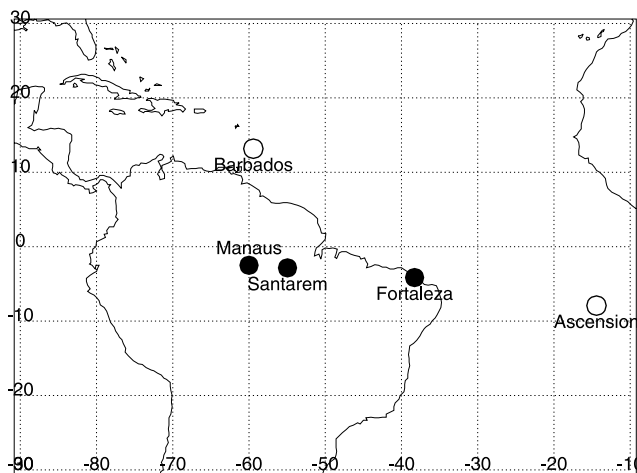


**Figure 1.** Map of sampling sites used in this study. Open circles are marine boundary layer (MBL) background sites and filled circles are vertical profile sites within Brazil.

use co-measured sulfur hexafluoride (SF<sub>6</sub>, a purely anthropogenic gas) as a transport tracer. Almost all SF<sub>6</sub> is emitted in the NH, and there are essentially no emissions of SF<sub>6</sub> between the coast and our sites [Olivier *et al.*, 1999]. Thus, all variations seen at our aircraft sites result from varying amounts of Northern and Southern Hemisphere tropical air arriving at our sites. Figure 2 shows that most of the time SF<sub>6</sub> at SAN and MAN is bounded by the time series from ASC and RPB. Using a simple two-end-member mixing model, we then calculate the fractions of air arriving at our Amazonian sites that can be represented by the background sites ASC and RPB, which can then be applied to any other conserved tracer (equations 1 and 2).

$$ASC_{site} = 1 - RPB_{site} = \frac{SF_{6,site} - SF_{6,RPB}}{SF_{6,ASC} - SF_{6,RPB}} \quad (1)$$

$$X_{bg} = ASC_{SAN} \times X_{ASC} + RPB_{SAN} \times X_{RPB} \quad (2)$$

$ASC_{site}$  and  $RPB_{site}$  are the respective fractions of air arriving at our Amazonian sites (MAN or SAN),  $SF_{6,site}$  is the median SF<sub>6</sub> from the vertical profile *site*, and  $SF_{6,(RPB \text{ or } ASC)}$  is the SF<sub>6</sub> mixing ratio extracted from a smoothed curve fit [Thoning *et al.*, 1989] of the background data at the same date as the *site* observations;  $X$  refers to the mixing ratio of any co-measured gas. We then calculate the enhancement above background by subtracting  $X_{bg}$  from measurements at all altitudes (Figure 3). Measurements of CH<sub>4</sub> at FTL show free troposphere (>1500 m) CH<sub>4</sub> enhancements of 10–20 ppb (Figure S2), indicating that it is not totally justified to use a single MBL-based point,  $X_{bg}$ , as a background for the entire 0 to 4 km range. However, the FTL enhancements are small compared to the Amazonian sites and only a few FTL profiles are available for reference, requiring us to use the temporally dense time series at ASC and RPB.

[10] Figure 3 shows the difference between vertical profile measurements of CH<sub>4</sub> at *site* (SAN or MAN) and the background as calculated in (2) for the dry and wet seasons. There is enhancement in the CBL, while in the free

<sup>1</sup>Auxiliary materials are available in the HTML. doi:10.1029/2006GL029213.

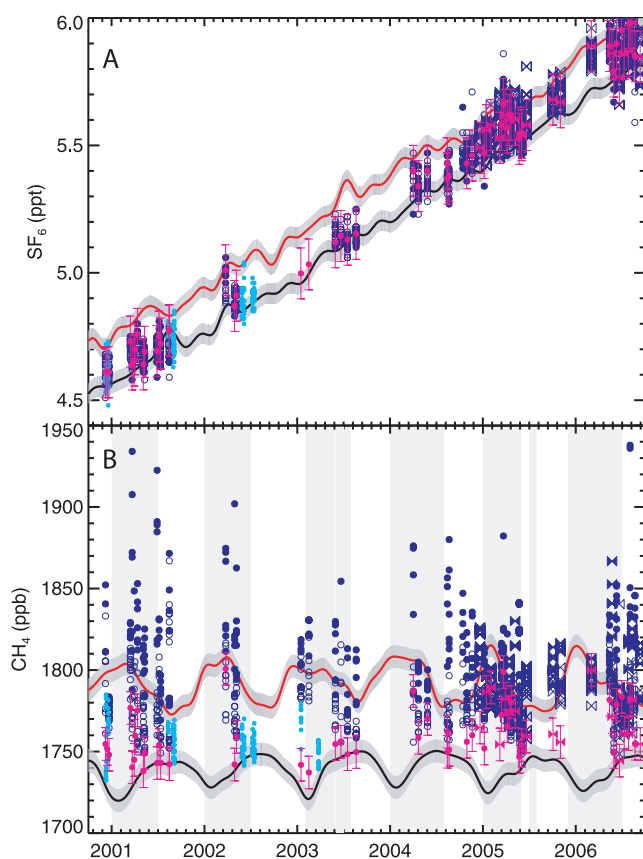


**Figure 2.** Time series of (a)  $\text{SF}_6$  and (b)  $\text{CH}_4$  at the marine boundary layer (MBL) sites ASC (black line) and RPB (red line), as well as the Brazilian vertical profile sites FTL (light blue circles), SAN (dark blue circles), and MAN (dark blue bowties). Filled symbols are those samples from lower than 1500 m and open symbols are above. Pink symbols and their uncertainties (one sigma) represent the calculated background value for a given vertical profile derived using  $\text{SF}_6$  measurements as discussed in the main text. The dark grey boundaries around the MBL time series are the uncertainties, which are standard deviation of the actual observations about the best-fit lines. For reference, the light grey vertical bars in Figure 2b show months at Santarém when rainfall exceeded 100 mm.

troposphere, values are both positive and negative. While positive free troposphere values are physically reasonable, the negative values are likely due to errors in our background subtraction and not  $\text{CH}_4$  sink processes. However, this also suggests that some of the free troposphere positive values also arise from errors in our background calculation. We do not adjust any profiles after background subtraction but instead allow this uncertainty to propagate into our flux calculations.

[11] The differenced profiles can be converted to surface fluxes by integrating the  $\text{CH}_4$  content from the surface to the top of the profile, and normalizing by the time since the air was at the coast, according to:

$$F_{\text{CH}_4} = \frac{\int_{z=0}^{4 \text{ km}} ([\text{CH}_4]_{\text{site}} - [\text{CH}_4]_{\text{bg}}) dz}{t} \quad (3)$$

where  $[\text{CH}_4]$  is the concentration of  $\text{CH}_4$  in  $\text{mol/m}^3$ , which can be determined from vertical profiles of mixing ratio, temperature and pressure (estimated using a lapse rate of 6.5 K/km and a scale height of 7 km).  $t$  is the time since the air has been over land, estimated using mean 850 mb windspeed of 10 m/s ([www.cdc.noaa.gov/cdc/data.ncep.html](http://www.cdc.noaa.gov/cdc/data.ncep.html)) and a mean distance to the coast of 1700 km (it is much less to the northeast and more to the southeast); we derive a mean value for  $t$  of 2 days, to which we assign a 50% uncertainty. Uncertainties in  $\text{SF}_6$  and  $\text{CH}_4$  values used in equations 1 and 2 are 0.05 ppt and 10 ppb, respectively, and are based on the scatter about smooth curve fits in Figure 2; uncertainty in  $[\text{CH}_4]_{\text{site}}$  in equation 3 is just the measurement uncertainty of 2 ppb. Uncertainty in  $F_{\text{CH}_4}$  as shown in Figure 4 is estimated by propagating uncertainty from all terms in equations 1–3. The sensitivity of  $F$  to possible biases is also tested and discussed below.

[12] Fluxes estimated using SAN data (Figure 4) average  $35 \pm 23 \text{ mg CH}_4/\text{m}^2/\text{day}$  and  $20 \pm 17 \text{ mg CH}_4/\text{m}^2/\text{day}$  at MAN. The mean uncertainty of each flux determination at SAN and MAN is 21 and 15  $\text{mg CH}_4/\text{m}^2/\text{day}$ , respectively. These integrated fluxes are significantly larger than any single flux averaged over a large area. Basinwide wetland emissions determined from chamber measurements and remote sensing [Melack *et al.*, 2004] of 29 Tg  $\text{CH}_4/\text{yr}$  distributed over  $5 \times 10^6 \text{ km}^2$  equate to 16  $\text{mg CH}_4/\text{m}^2/\text{day}$ . Scaling direct plant emissions from laboratory chambers is uncertain [Ferretti *et al.*, 2007; Houweling *et al.*, 2006; Keppler *et al.*, 2006; Kirschbaum *et al.*, 2006], but here we use 4  $\text{mg CH}_4/\text{m}^2/\text{day}$  (see auxiliary material); nighttime emissions of unknown origin measured at upland Amazonian sites [do Carmo *et al.*, 2006] have a median of about 5  $\text{mg CH}_4/\text{m}^2/\text{day}$ , but if they are plant emissions, they could be significantly larger in the presence of sunlight [Keppler *et al.*, 2006]. Maximum fire emissions over a five year period from 65°W to the Atlantic coast between 5°S and the equator are estimated to be  $5 \times 10^{10} \text{ g CH}_4/\text{month}$  (G. van der Werf, personal communication, 2006). If we assume that fires occur one third of the days during the dry season, this equates to 5  $\text{mg CH}_4/\text{m}^2/\text{day}$  for days when fires occur. Termite sources (0.5  $\text{mg}/\text{m}^2/\text{day}$ ) [Martius *et al.*, 1993], consumption by soils (<1  $\text{mg}/\text{m}^2/\text{day}$ ) [Keller *et al.*, 2005], and consumption by OH (3  $\text{mg}/\text{m}^2/\text{day}$ ), also likely contribute. No individual process estimates can explain our mean values of 35 and 20  $\text{mg CH}_4/\text{m}^2/\text{day}$  based on SAN and MAN observations, but all sources and sinks total 23  $\text{mg CH}_4/\text{m}^2/\text{day}$ , closer to our observations. Wetland emissions are likely to be the most important source in the wet season, while during the dry season a combination of wetland, fire and other sources influence the observed  $\text{CH}_4$  enhancements. We do not presently have a way of distinguishing direct-plant and wetland emissions, so at present we assume emissions from plants that are uniform throughout the year.

[13] One potential experimental bias is whether our air samples are representative of large areas or just the area near the sampling sites. There is no consistent bias between our two profiles taken 30 km apart (Figure S1), although there is significant spread at the lowest level suggesting some influence from local fluxes. Re-calculating fluxes using the non-tower profiles or by not using the lowest two (300 and 600 m) levels reduces the mean flux at the sites

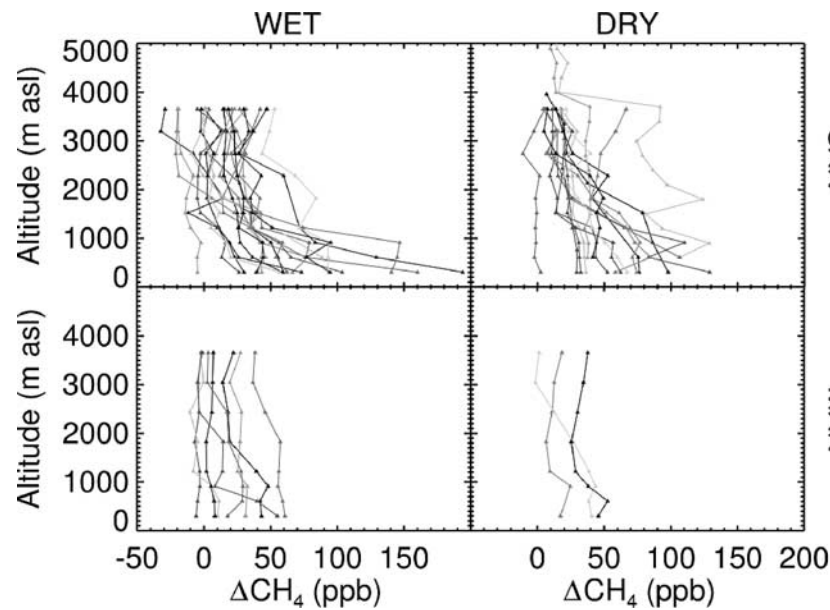


**Figure 3.**  $\text{CH}_4$  vertical profiles from (top) SAN and (bottom) MAN during the (left) wet and (right) dry seasons, differenced from a marine boundary layer reference as discussed in the text. Different shades of gray represent profiles collected on different days and are included as a visual aid to separate profiles.

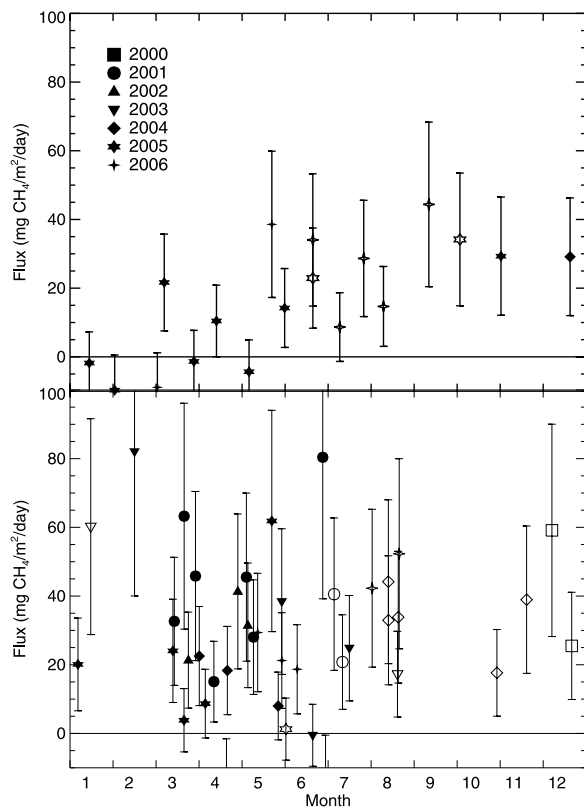


**Figure 4.** Estimated methane fluxes at (top) MAN and (bottom) SAN for all years. Uncertainties are one standard deviation derived by propagating uncertainty in all terms of equations 1, 2, and 3. Filled symbols are fluxes during months of greater than 100 mm rainfall and open symbols less than 100 mm.

by only 0–5  $\text{mg CH}_4/\text{m}^2/\text{day}$ , indicating that most of the integrated signal is not local ( $\sim 10^2 \text{ km}^2$ ), but regional ( $\sim 10^5 \text{ km}^2$ ).

[14] Bias may also result from our measurements not exceeding about four km. Due to convection, some methane emissions will affect the profile above this height, and neglecting these altitudes will result in an underestimate of emissions. On the other hand, free troposphere FTL data show enhancements of about 15 ppb above two km (relative to the MBL); this translates to a positive bias of 6  $\text{mg CH}_4/\text{m}^2/\text{day}$  (assuming two days travel time from FTL to SAN). Neglecting destruction of  $\text{CH}_4$  introduces a negative bias of about 3  $\text{mg CH}_4/\text{m}^2/\text{day}$  in a column from the surface to 4 km.

#### 4. Conclusions

[15] We interpret our measurements as a “climatological Lagrangian experiment,” such that the mean fluxes are more reliable than any single flux determination. This is appropriate for our estimation strategy which intentionally avoids the use of detailed models of atmospheric transport, but instead relies upon the position of our measurement sites relative to the strong easterly trade winds. Furthermore, our use of  $\text{SF}_6$  as tracer of Northern and Southern Hemisphere air allows us to improve the accuracy of our boundary condition calculation relative to using data from just a single site, like ASC. In the future, our observations can be used with detailed models of atmospheric transport to make more highly resolved estimates of surface  $\text{CH}_4$  fluxes in eastern Amazônia.

[16] **Acknowledgments.** This project was conducted under the Brazilian-led Large-scale Biosphere-atmosphere experiment in Amazônia (LBA), and funded from NASA inter-agency agreements S-10137 and S-71307. We thank Michael Hahn, Doug Guenther, Aaron Watson, Kirk Thoning, Patricia Lang, Liliane Polakiewicz, and Elaine Martins for assistance in sampling, analysis, and data processing.

## References

- Andreae, M. O., and P. Merlet (2001), Emission of trace gases and aerosols from biomass burning, *Global Biogeochem. Cycles*, *15*(4), 955–966.
- Bergamaschi, P., et al. (2006), Satellite cartography of atmospheric methane from SCIAMACHY onboard ENVISAT: 2. Evaluation based on inverse model simulations, *J. Geophys. Res.*, *112*, D02304, doi:10.1029/2006JD007268.
- Bousquet, P., et al. (2006), Contribution of anthropogenic and natural sources to atmospheric methane variability, *Nature*, *443*(7110), 439–443.
- Cicerone, R. J., and R. S. Oremland (1988), Biogeochemical aspects of atmospheric methane, *Global Biogeochem. Cycles*, *2*, 299–327.
- Conway, T. J., P. P. Tans, L. S. Waterman, K. W. Thoning, D. R. Kitzis, K. A. Masarie, and N. Zhang (1994), Evidence for interannual variability of the carbon cycle for the National Oceanic and Atmospheric Administration/Climate Monitoring Diagnostics Laboratory Global Air Sampling Network, *J. Geophys. Res.*, *99*(D11), 22,831–22,855.
- Dlugokencky, E. J., R. C. Myers, P. M. Lang, K. A. Masarie, A. M. Crotwell, K. W. Thoning, B. D. Hall, J. W. Elkins, and L. P. Steele (2005), Conversion of NOAA atmospheric dry air CH<sub>4</sub> mole fractions to a gravimetrically prepared standard scale, *J. Geophys. Res.*, *110*, D18306, doi:10.1029/2005JD006035.
- do Carmo, J. B., M. Keller, J. D. Dias, P. B. de Camargo, and P. Crill (2006), A source of methane from upland forests in the Brazilian Amazon, *Geophys. Res. Lett.*, *33*, L04809, doi:10.1029/2005GL025436.
- Ferretti, D. F., J. B. Miller, J. W. C. White, K. R. Lassey, D. C. Lowe, and D. M. Etheridge (2007), Stable isotopes provide revised global limits of aerobic methane emissions from plants, *Atmos. Chem. Phys.*, *7*, 237–241.
- Frankenberg, C., J. F. Meirink, P. Bergamaschi, A. P. H. Goede, M. Heimann, S. Körner, U. Platt, M. van Weele, and T. Wagner (2006), Satellite cartography of atmospheric methane from SCIAMACHY on board ENVISAT: Analysis of the years 2003 and 2004, *J. Geophys. Res.*, *111*, D07303, doi:10.1029/2005JD006235.
- Houweling, S., T. Kaminski, F. Dentener, J. Lelieveld, and M. Heimann (1999), Inverse modeling of methane sources and sinks using the adjoint of a global transport model, *J. Geophys. Res.*, *104*(D21), 26,137–26,160.
- Houweling, S., T. Röckmann, I. Aben, F. Keppler, M. Krol, J. F. Meirink, E. J. Dlugokencky, and C. Frankenberg (2006), Atmospheric constraints on global emissions of methane from plants, *Geophys. Res. Lett.*, *33*, L15821, doi:10.1029/2006GL026162.
- Keller, M., R. Varner, J. D. Dias, H. Silva, P. Crill, and R. C. de Oliveira (2005), Soil-atmosphere exchange of nitrous oxide, nitric oxide, methane, and carbon dioxide in logged and undisturbed forest in the Tapajós National Forest, Brazil, *Earth Interact.*, *9*, 1–28.
- Keppler, F., J. T. G. Hamilton, M. Braß, and T. Rockmann (2006), Methane emissions from terrestrial plants under aerobic conditions, *Nature*, *439*(7073), 187–191.
- Kirschbaum, M. U. F., D. Bruhn, D. M. Etheridge, J. R. Evans, G. D. Farquhar, R. M. Gifford, K. I. Paul, and A. J. Winters (2006), A comment on the quantitative significance of aerobic methane release by plants, *Funct. Plant Biol.*, *33*(6), 521–530.
- Lloyd, J., et al. (2001), Vertical profiles, boundary layer budgets, and regional flux estimates for CO<sub>2</sub> and its <sup>13</sup>C/<sup>12</sup>C ratio and for water vapor above a forest/bog mosaic in central Siberia, *Global Biogeochem. Cycles*, *15*(2), 267–284.
- Martius, C., R. Wassmann, U. Thein, A. Bandeira, H. Rennenberg, W. Junk, and W. Seiler (1993), Methane emission from wood-feeding termites in Amazonia, *Chemosphere*, *26*(1–4), 623–632.
- Melack, J. M., L. L. Hess, M. Gastil, B. R. Forsberg, S. K. Hamilton, I. B. T. Lima, and E. Novo (2004), Regionalization of methane emissions in the Amazon basin with microwave remote sensing, *Global Change Biol.*, *10*(5), 530–544.
- Miller, J. B., K. A. Mack, R. Dissly, J. W. C. White, E. J. Dlugokencky, and P. P. Tans (2002), Development of analytical methods and measurements of <sup>13</sup>C/<sup>12</sup>C in atmospheric CH<sub>4</sub> from the NOAA Climate Monitoring and Diagnostics Laboratory Global Air Sampling Network, *J. Geophys. Res.*, *107*(D13), 4178, doi:10.1029/2001JD000630.
- Olivier, J. G. J., A. F. Bouwman, J. J. M. Berdowski, C. Veldt, J. P. J. Bloos, A. H. J. Visschedijk, C. W. M. van de Maas, and P. Y. J. Zandveld (1999), Sectoral emission inventories of greenhouse gases for 1990 on per country basis as well as on 10 × 10, *Environ. Sci. Policy*, *2*, 241–264.
- Richey, J. E., J. M. Melack, A. K. Aufdenkampe, V. M. Ballester, and L. L. Hess (2002), Outgassing from Amazonian rivers and wetlands as a large tropical source of atmospheric CO<sub>2</sub>, *Nature*, *416*(6881), 617–620.
- Tans, P. P., P. S. Bakwin, and D. W. Guenther (1996), A feasible global carbon cycle observing system: A plan to decipher today's carbon cycle based on observations, *Global Change Biol.*, *2*(3), 309–318.
- Thoning, K. W., P. P. Tans, and W. D. Komhyr (1989), Atmospheric carbon dioxide at Mauna Loa Observatory: 2. Analysis of the NOAA GMCC data, 1974–1985, *J. Geophys. Res.*, *94*(D6), 8549–8565.
- Walter, B. P., M. Heimann, and E. Matthews (2001), Modeling modern methane emissions from natural wetlands: I. Model description and results, *J. Geophys. Res.*, *106*(D24), 34,189–34,206.

P. Artaxo, Instituto de Física, Universidade de São Paulo, Caixa Postal 66318, CEP 05315-970 São Paulo, SP, Brazil.

P. Bakwin, A. M. Crotwell, E. J. Dlugokencky, J. B. Miller, and P. P. Tans, NOAA Earth System Research Laboratory, 325 Broadway, Boulder, CO 80303, USA. (john.b.miller@noaa.gov)

M. T. S. d'Amelio and L. V. Gatti, Divisao de Quimica Ambiental, Laboratorio de Quimica Atmosferica, Insituto de Pesquisas Energéticas e Nucleares, Av. Lineu Pretes, 2242, Cidade Universitaria, CEP 05508-900 São Paulo, SP, Brazil.